Alzheimer's disease stage prediction using a novel transfer learning-Alzheimer's network architecture

Pothala Ramya[1,2], Chappa Ramesh[3], Odugu Srinivasa Rao[1]
[1]Department of Computer Science and Engineering, JNTUK University, Kakinada, India
[2]Department of Information Technology, MVGR College of Engineering, Vizianagaram, Inida
[3]Department of Computer Science and Engineering, Aditya Institute of Technology and Management, Tekkali, India

Article Info

ABSTRACT

The root cause of Alzheimer's disease (AD) is unknown except for a very tiny number of family instances caused by a genetic mutation. A thorough examination of particular brain disorders' tissues is necessary to correctly identify the circumstances using scans of magnetic resonance imaging (MRI), and specific non-brain tissues, like the neck, skin, muscle, and fat, make further investigation challenging and can be seen in MRI scans. This work aims to use the FSL-BET skull stripping tool to remove non-brain tissues and extract the significant region of the brain- deep learning (DL) techniques rather than machine learning (ML) models helpful in classification and predictions. The most frequent issue with DL models is which needs a lot of training data, causes to problems with class imbalance. To avoid imbalance issues, we used data augmentation to ensure that the samples were distributed equally among the classes. A novel transfer learning Alzheimer's disease network (TL-AzNet) based visual geometry group-19 (VGG19) technique was developed in this study. Conducted a comparison study using the base and suggested models, comparing over data with oversampling versus non-oversampling. The novel model predicted AD with a 95% accuracy rate.

Corresponding Author:

Pothala Ramya
Department of Computer Science and Engineering, JNTUK University
Kakinada, Andhra Pradesh, India
Email: ramya.p@mvgrce.edu.in

1. INTRODUCTION

Alzheimer's disease (AD) is marked by genetic signs such as tau-containing neurofibrillary tangles and plaques with β-amyloid [1]. It's a 50% inheritable ailment cognitive impairment, periodically occurred AD [2], [3]. It mainly araises in mid ages and late lifes, main risk for men over 45 than women, over 65 [4]. Deep learning (DL) approaches proven that they are successful in several healthcare applications because they can autonomously acquire hierarchical representations from intricate data [5].

In this research, utilizing an oversampling technique known as data augmentation. we employed the pre-trained visual geometry group-19 (VGG19) model to automatically classify brain MRI scans and diagnose the phases of AD. This Studey main job is to develop a novel transfer learning Alzheimer's disease network (TL-AzNet) model using the VGG19 base DL model. To handle the limitation of insufficient data samples, analysed the significance of utilizing the features of natural images to categorize medical images [6], [7]. The key contributions are [8]. i) We developed a TL based method that utilizes a pre-trained model to perfectly diagnose different stages of AD using MRI scans. ii) Addressing the issue of uneven data sample distribution by employing data augmentation techniques with various parameters.

iii) Employing both the primary and three-dimensional perspectives of brain MRI scans to categorize different stages of dementia.

An *et al.* [9] developed 3-layers for ensemble learning associated with DL architecture. Two sparse auto-encoders trained at one layer i.e voting. 2nd layer is the optimal layer uses over-sampling techniques and thresholds. 3rd is a stacking layer uses a deep belief network with features like nonlinear weighted techniques. Gathered the dataset from NACC-UDS and applied it to six ensemble approaches for better predictions of AD. Nguyen *et al.* [10] proposed a hybrid learning framework. This hybrid learning used 3D-residual network (ResNet) with ADNI imagining data and extreme gradient boosting (XGBoost) to analyze the voxel-by-voxel-based images to identify voxel groups. 100% AUC is achieved at the training phase and 96% on testing. Created a strategy that mixes ensemble training with a 3D Conv network. When confirming AD, with ADNI-MRI data generated an accuracy of 95.2% in discerning between AD and NC (standard control) cases and 77.8% in separating between stable mild cognitive impairment (sMCI) and progressive mild cognitive impairment (pMCI) cases [11]. Mohammad and Al Ahmadi [12] included VGG19 DL model. A comprehensive feature map is accomplished by mixing with top level features of fc7-8 layers of VGG19. Utilized an optimestic WoA-whale optimization algorithm, for optimizing and choosing most leading features. Latter the F-KNN algorithm achieved 99% pr:precision. Khan *et al.* [13] developed a model with transfer learning (TL) considered ADNI: 4 performed image segmentation to set apart GM (grey matter) from image because it's a crucial part to predict AD—used a pre-trained VGG model to fine-tune obtained 97% accuracy. Afzal *et al.* [14] utilized OASIS data augmentation to prevent imbalance issues. This study employed a TL approach with 3D-MRI achieved an accuracy of 98% on single-view images, 3D views achieve 95% accuracy. Raza *et al.* [15] included three components: grey matter (GM) 2D, white matter (WM), and cerebrospinal fluid (CSF), using the SPM12 software for preprocessing. A pre-trained DenseNet model was used to analyze the segmented GM slices, with the last two blocks being retrained with an accuracy of 97.84% in the multiclass classification of AD. Balaji and Veni [16] used brain extraction or skull stripping tools, manual extraction takes 60 min's They performed comparisons using different tools and models like BET2, RoBEX, and UNet3D. The proposed model demonstrates strong competency with a dice score of 98%, surpassing the UNet3D model by 1%. Stoleru and Iftene [17] utilized ResNet-152 and AlexNet as transfer-learning deep model and skull stripping ADNI sagittal image set data. ResNet-152: 99% accuracy and AlexNet: achieves 98% accuracy [17]. Wang *et al.* [18] introduces Deephipp included 3D dense block and an attention mechanism to segment the hippocampus precisely. (i) data augmentation (ii) 3D dense block (iii) DeepHipp applies the attention process. The fortune of DeepHipp showcases its capability to attain an accuracy of 83.63%.

Earlier studies investigated CNN and other DL architectures for AD image categorization, achieved great success but frequently call for huge labelled datasets and a lot of processing power. Due to variability in imaging procedures, current models may fail to generalizing across a variety of datasets. We suggest a novel TL-AzNet design to overcome these issues. Our method reduces the requirement for large amounts of training data while enhancing feature extraction and classification performance by incorporating TL techniques.

The remaining sections of this work are put in order as: section 2 gives an extensive description of the suggested TL-AzNet model for AD classification. The study presents the evaluation of the proposed model alongside the state-of-the-art model in section 3. The last section, section 4, finishes the paper by discussing future aims.

2. METHOD

The pre-processed dataset was collected from Kaggle and adopted to train recommended and prior acquired ways for the safe and exact identification of AD. Figure 1 provides an explanation of various phases involved in suggested architecture workflow.

2.1. Dataset descripton

It's four class datasets about Alzheimer's illness utilized the Kaggle repository samples. The Table 1 provides information on the spreading of 6400 MRI pictures and the mean (average) and SD-standard deviation of the mini-mental state exam (MMSE) score. The MMSE results assess the range of dementia severity. There are 30 questions, so the maximum achievable score is 30. This test calculates the total number of accurate responses given by the patients. Figure 2 shows how they appeared in the dataset directories of the all-class images.
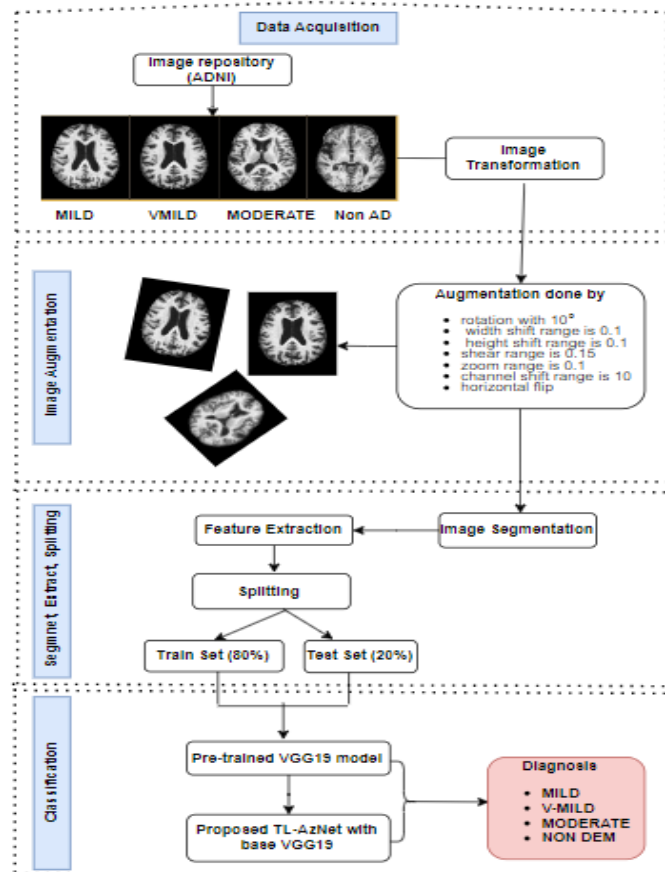
Figure 1. Proposed workflow structure to predict multiclass

Table 1. Shows mean, StandDev-MMSE results between classes

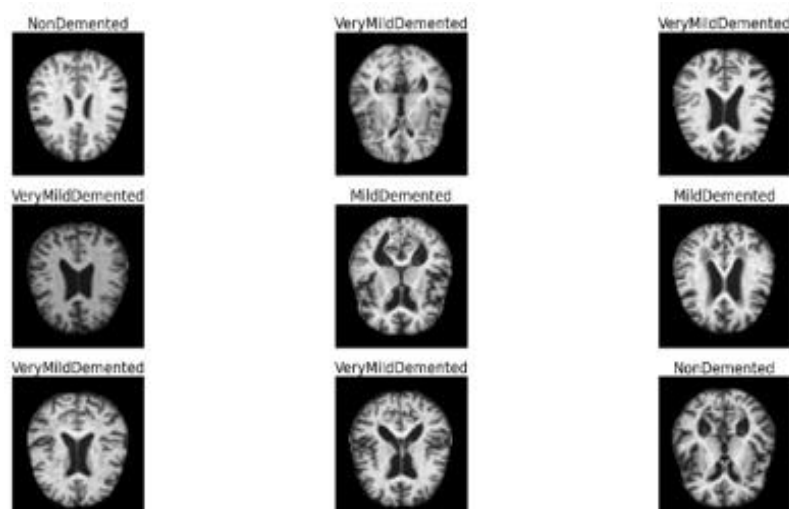| Group	Image subject	No. of patients	Mean MMSE	Stand deviation of MMSE
ND	3,200	100	23.50	5.10
VMD	2,240	70	24.51	5.28
MID	896	28	25.12	4.90
MOD	64	2	21.77	2.67

Figure 2. Samples of the multiclass dataset

As the extremity of dementia worsens, Figure 3 exhibits the arithmetical properties of the images, such as mean, standard deviation, and skew, tend to group within a narrower range. Moreover, there is a noticeable increase in skewness as severity increases. Even if, these observations not ultimate results which indicate that utilizing these statistical characteristics could enhance and accelerate the training procedure of a DL model [19].
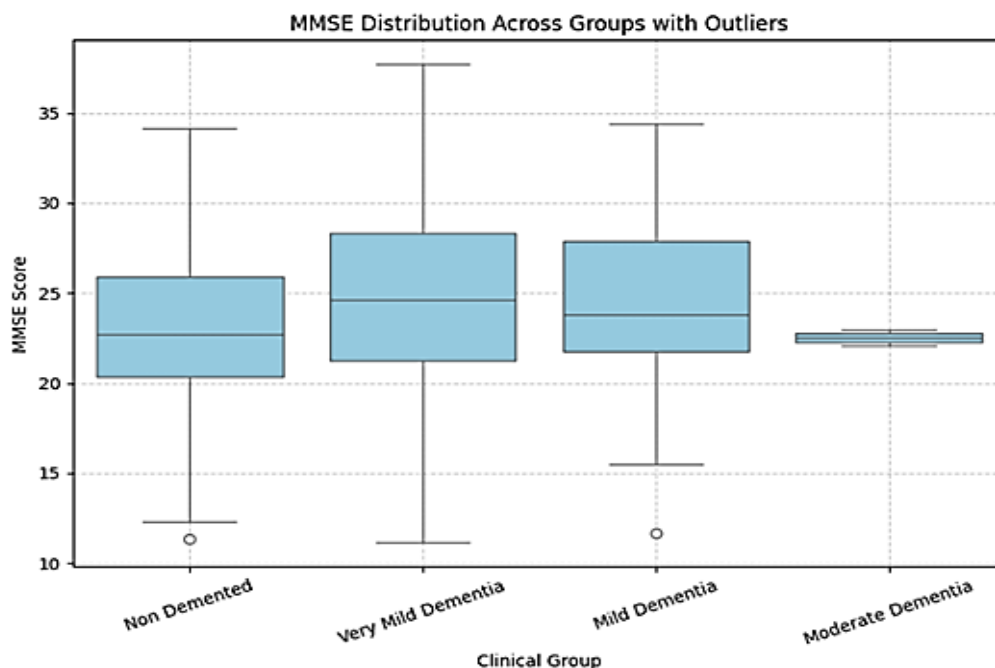

Figure 3. Shows statistical analysis of classes using box plot

2.2. Preprocessing

We are facing an imbalance issue based on the class distribution shown above. The non-demented MRI class accounts for 50% of the dataset, comprising 3,200 images. In contrast, the moderate demented MRI class represents only 1% of the dataset, comprising 64 images. Data augmentation can prevent this [20]. The machine learning models fail to tackle the imbalance problem. So, in order to handle this issue, we are moving towards DL. The formula below shows how the sample is distributed using the class weight formula. The formula for class weights,

class_weight = (Total Number of images/Number of class x Images per class)

Weight for class "Mild_Demented": 1.79, "Moderate_Demented": 25.0, "Non_Demented": 0.5 "Very_Mild_Demented": 0.71. Moderate_Demented has a high-class weight threshold value, which indicates it is a minority class. We need to increase the number of image samples in Moderate_Demented [21].

2.3. Data augmentation

Data augmentation can mainly be used to overcome the issue of overfitting. It can be elevated when there is deficient data to train the model, leading to a challenge for its accuracy [22]. This research uses rescaling pixel values, adjusting brightness, changing magnification levels, filling in newly formed pixels with a constant value, and randomly flipping images horizontally to pass as parameters to produce image copies appeared in Figure 4. The Table 2 showing comparison of class distribution before and after August across MID, MOD, ND, and VMD catagories.

Table 2. Shows before aug and after aug to balance the MRI data

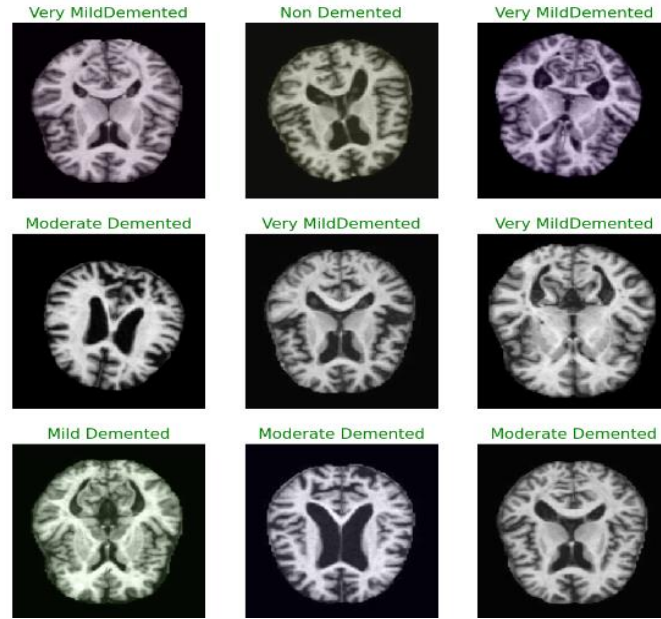| No. of class	MID	MOD	ND	VMD
Before Aug	896	64	3200	2240
After Aug	7258	7040	7400	7392

Figure 4. Shows data augmentation image samples

2.4. Feature extraction

It came into picture for identifying and representing the significant components of a images in a concise feature vector. The initial layers of a deep network, specifically the convolution layer, implicitly represent image information. These features are defined by the formats of the filters employed in the network. Calculate the output volume by applying specific parameters as a function of the input volume size. To create a valid convolutional layer, it is necessary to ensure the following:

$$W_0 = \frac{(W_i - FK + 2P)}{S} + 1 \tag{1}$$

$$H_0 = \frac{(H_i - FK + 2P)}{S} + 1 \tag{2}$$

$$D_0 = K \tag{3}$$

- W_o width of output Volume, W_i input volume.
- H_o height of output volume, H_{igh} input volume.
- D_o Dropout.
- FK kernel size.
- S is stride.
- P is the amount of zero padding.

The pooling layer operates independently on each depth section of the input and rescales its size by performing the MAX operation. The system determined the dimensions of the HDW volume and then partitioned the image into segments.

$$W_0 = \frac{(W_i - F)}{S} + 1 \tag{4}$$

$$H_0 = \frac{(H_i - F)}{S} + 1 \tag{5}$$

2.5. Skull stripping

Skull-stripping, eliminates non-brain tissue connections from MRI data. The brain extraction tool (BET) utilizes a deformable model that gradually adjusts to conform to the brain's surface through a series of locally adaptive model forces. BET does an intensity-based estimation to identify the threshold for brain and non-brain regions. It calculates the head's centre of gravity and uses it to define an initial sphere [23]. Figure 5 epresses skull separation like sphere is then expanded until it reaches the edge of the brain.
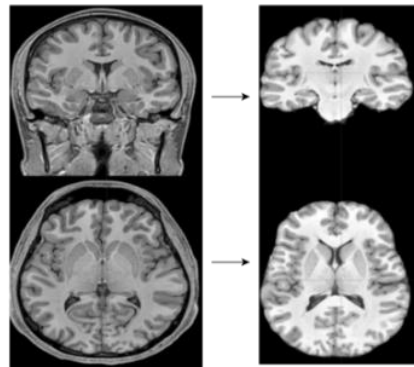
Figure 5. Shows the original high-resolution image and their corresponding brain extracted image

2.6. Explainability methods

Several flawed reasoning scenarios were included in this study, such as: i) Image quality: low-quality images can produce false-negative results in early-stage dementia. ii) Overlapping features: in very mild to no dementia, hippocampal and cortical atrophy may be similar to normal aging. When comparing mild vs. moderate dementia, it is difficult to categorize borderline cases.

Several best-case explanation techniques were used to interpret the model's decisions regarding early AD detection, as shown in Figure 6. Figures 6(a)-6(d) demonstrate how these techniques can help address the aforementioned issues. i) Grad-CAM: creates a heatmap identifying key regions in the image below; green circles represent the hippocampus and blue circles represent cortical regions. ii) SHAP: SHapley additive explanation, finding clinical and genetic biomarkers and early disease diagnosis will greatly benefit from this. iii) LIME: better diagnosis through knowledge of the most important aspects for prognosis.
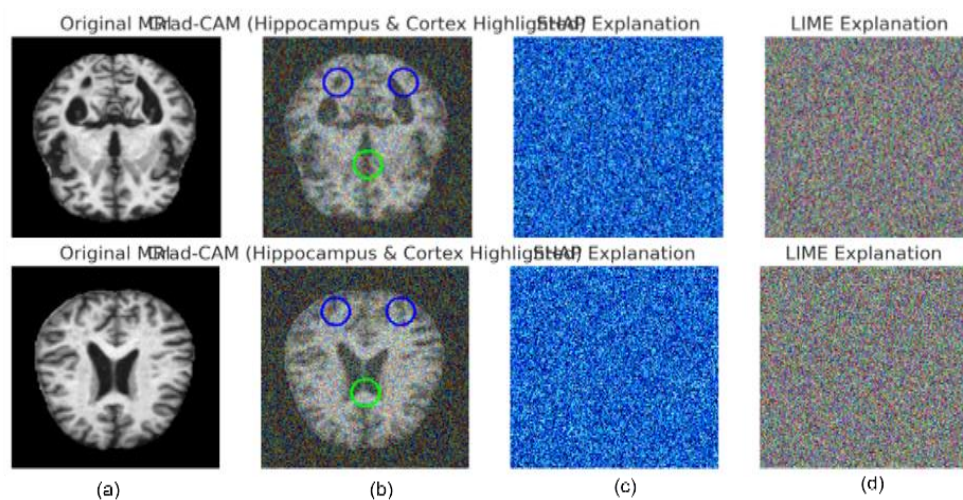

Figure 6. Represents identification of key biomarkers for early-stage AD prediction: (a) original MRI Scan, (b) Grad-CAM (Hippocampus, Cortical Regions), (c) SHAP, and (d) LIME

2.7. Proposed method

The TL-AzNet model, which utilizes a VGG19 (16-CNN and 3-FC) base deep-CNN. TL involves employing a preexisting generic model and subsequently retraining it with our specific dataset, which can simplify the process. The model consists of many layers that carry out four fundamental operations: convolution, maxpooling, flattening, and dense [24].

i)   Convolution layer 1, 2, 3, 4, and 5: these are primary component of DL models, Conv1 is an input layer with 2D images (3×3×3-> width, height, depth), 224×224 size fed to TL-AzNet. The starting CNN layer sizes are 128, 256, and 512, respectively. 1D Max pooling (2×2×2) layer and ReLu as activation function. It creates a feature map with 64 batch size to dlattened dense layer [25].

ii) Output layer: SoftMax is the output layer, which produces the highest probability vector at each hidden layer. 70% training, data from seven tags in each zone were utilized, whereas 30% testing, data from three tags in each zone were used. We conducted a grid search Table 3. determines the ideal values for the number of hidden units, dropout rate, learning rate, and batch size.

After setting the all necessary filters and tuning params the Figures 7 and 8 presents recommended model architecture and output shapes of each layers with params range.

Table 3. Shows recommende model fine-tune parameters and values

Fine-tuned parameters	Values
Acti fun	ReLu
Epochs	30, 50, 100
Batch size	128
Optimizer	Adam
Loss function	Categorical cross entropy
Drop out	0.2
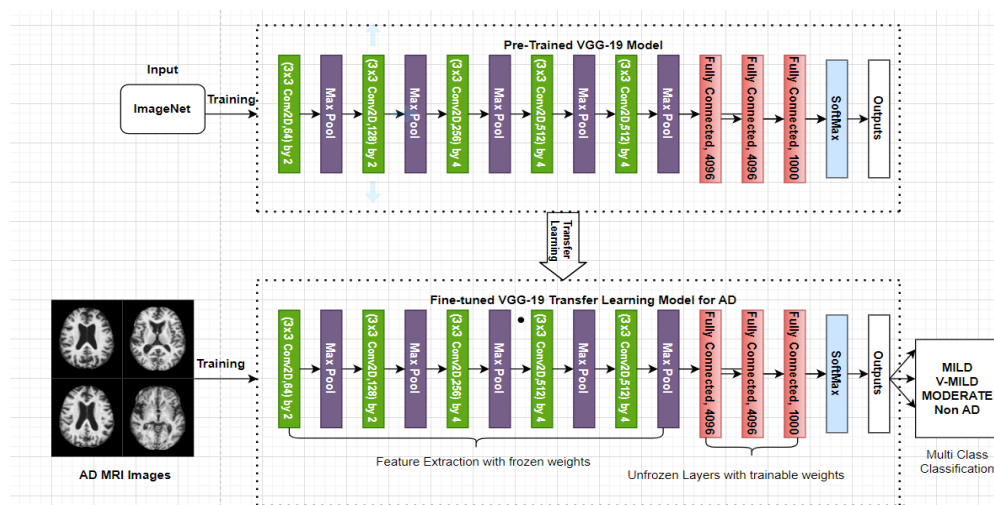
Figure 7. Proposed model architecture

Layer name	#Filters	#Parameters	#Activations
input			150K
conv1_1	64	1.7K	3.2M
conv1_2	64	36K	3.2M
max pooling			802K
conv2_1	128	73K	1.6M
conv2_2	128	147K	1.6M
max pooling			401K
conv3_1	256	300K	802K
conv3_2	256	600K	802K
conv3_3	256	600K	802K
conv3_4	256	600K	802K
max pooling			200K
conv4_1	512	1.1M	401K
conv4_2	512	2.3M	401K
conv4_3	512	2.3M	401K
conv4_4	512	2.3M	401K
max pooling			100K
conv5_1	512	2.3M	100K
conv5_2	512	2.3M	100K
conv5_3	512	2.3M	100K
conv5_4	512	2.3M	100K
max pooling			25K
fc6		103M	4K
fc7		17M	4K
output		4M	1K

Figure 8. Shows output shape and parameters of trainable and untrainable proposed model

The process of the suggested TL-AzNet model for AD stage classification is described in Algorithm 1. The backbone of the TL-AzNet architecture is a pre-trained VGG19 model, and its lower layers are frozen or fine-tuned to apply TL.

Algorithm 1. The proposed algorithm
```
1. BEGIN
2. INPUT: augmented dataset_directory.
3. model_parameters ← conv2D, max pool, flatten, Dense layers and Load data from
dataset_directory
4. break the whole set into training set and validation set with 80, 20%
5. Instantiate an ImageDataGenerator object for preprocessing
6. IF to use pre-formed model THEN
     1. model←Load pre-load VGG19 model
     2. ENDIF
7. TL-AzNet_model←apply transfer learning to model.
     1. freeze or fine-tune the bottom layers of TL-AzNet_model.
8. Compile the new model using Adam and categorical_crossentropy
9. Train the model on 100 epochs with a compiled model
10. metrics←[recall, precision, accuracy, AUC, f1-score, con_matrix]
11. FOR iterated on all-epochs of phase of training, DO
     1.       estimate the model staging, operate metrics with validation set
     2.            IF the accuracy is not raising with valid-set, THEN
     3.                 change values of Hyper-parameters (learning rate)
     4.            ENDIF
     5. ENDFOR
12. check the final model and evaluate performance using metrics
13.  OUTPUT: comparison between the recommended method and previous methods.
      1. prediction: four classifications [MILD, V-MILD, MODERATE, Non-AD]
14. END
```

3.   RESULTS AND DISCUSSION

TL-AzNet was inculcated on the dataset and 10-fold cross-validation. The interpretation of a model is mainly shown in terms of the confusion matrix. The new fine-tuned TL model with VGG19 base used to optimize the performance using metrics and iterated over 100 epochs. Table 3 presents which model is best fits to diagnosis the disease based on below evaluation.

i) Precision: it is a predictive class to identify probability of correct optimistic prediction.

$$pr = \frac{tf}{tp+fp} \tag{6}$$

ii) Recall: call it as sensitivity (SN), has a capacity to identify effected disease patients.

$$re = \frac{tp}{tp+fn} \tag{7}$$

iii) F1 score: used to measure test accuracy takes both the pr and re of the test sample.

$$f1-m = \frac{tp}{tp+\frac{1}{2}(fp+fn)} \tag{8}$$

iv) Accuracy: accuracy (acc) is reckoned on correct positive and negative predictions.

$$acc = \frac{tp+tn}{tp+fn+tn+fp} \tag{9}$$

We employed two techniques to prevent data leaks in order to guarantee an impartial assessment: i) Patient-level splitting: this can be used when the model performance is overestimated due to leak, it ensures that all scans of same patient belong to a single set (training, validation, or testing) rather than randomly splitting. ii) K-fold cross-validation was employed in conjunction with Subject Holdout to make sure that scans from the same patient did not show up in more than one-fold. The Table 4 shows the performance comparison across several training epochs between TL-Net model and the baseline VGG19 model. Additionally, it shows how TL and data augmentation can improve the classification of AD stage.

After evaluation, Figure 9 shows the confusion matrix. Figures 9(a) and 9(b) illustrate the proportion of reliable and unreliable estimates from the suggested model generated across the four classes. Figure 10. Depicts different visual graphs, representing the error and accuracy incurred by the suggested model over several epochs. The accuracy of the dataset achieves better performance with 100 epochs. Before augmentation, there was a severe misclassification for moderate dementia (64 samples) due to class

imbalance. After augmentation, the misclassification reduced with a balanced dataset. The cases of misclassification are as follows: i) 30 dementia cases were misclassified as moderate dementia. ii) 15 very mild dementia cases were misclassified as moderate dementia. iii) 68 mild dementia cases were misclassified as very mild dementia. iv) 10 moderate dementia cases were misclassified as very mild dementia.

Misclassification rates (following augmentation) both, i) mild dementia (3.55%) and ii) very mild dementia (2.77%) exhibit moderate categorization, most likely as a result of comparable patterns of brain atrophy. iv) non-dementia: 4.05% is the greatest rate, suggesting that some overlap with early stages of dementia. iii) moderate dementia: 1.99% is the lowest rate, which performs better as a disease classification. Figure 11. Identifies a class image lable is truly predicted after testing or not. Figure 12 depicts a bar plot between various classification models and their accuracies respectively. The Table 5 enumerates the comparison of various DL techniques for predicting AD across several datasets.

Table 4. Performance evaluation of the proposed model and VGG19 base model

Models	Epochs	Accuracy	F-score	Recall	Precision
VGG19 (without DA)	20	80	60	60	60
	50	90	83	70	90
	100	83	81	84	86
TL-Net (with DA)	20	81	59	60	60
	50	92	85	75	95
	100	95	95	94	96

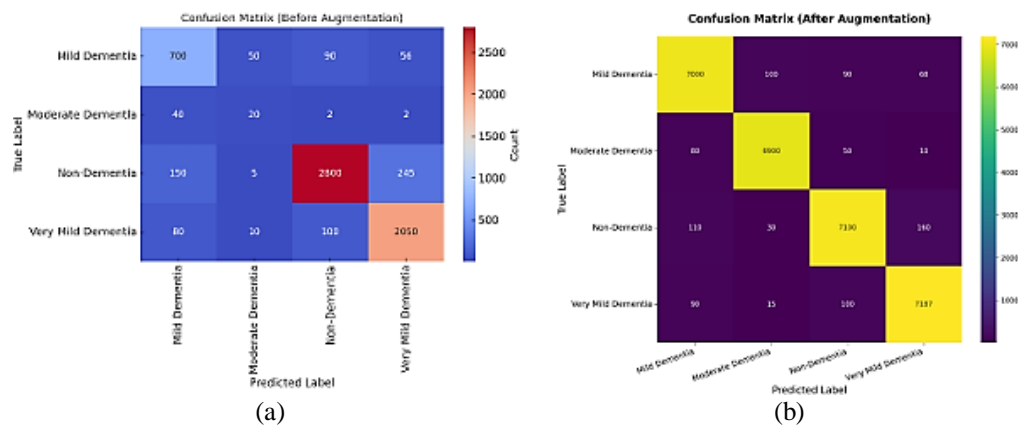(a)   (b)

Figure 9. Confusion matrix (a) before augmentation and (b) after augmentation
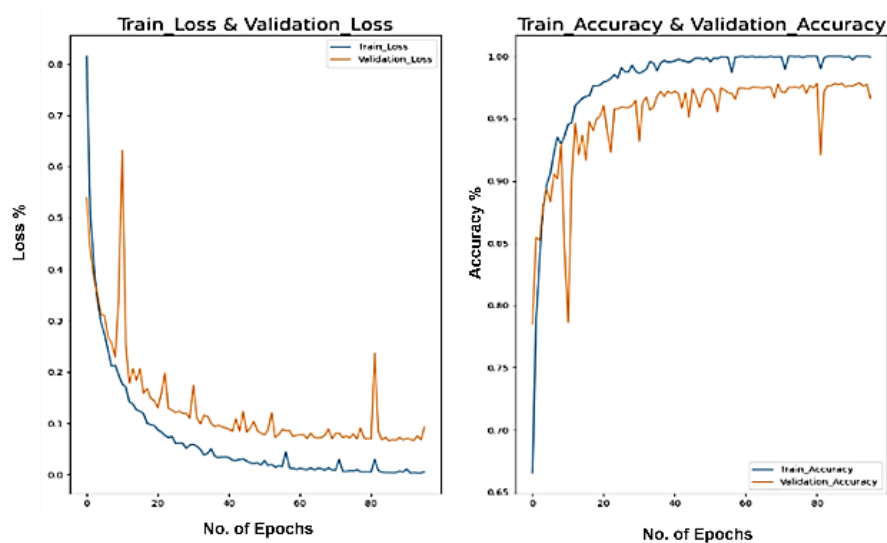

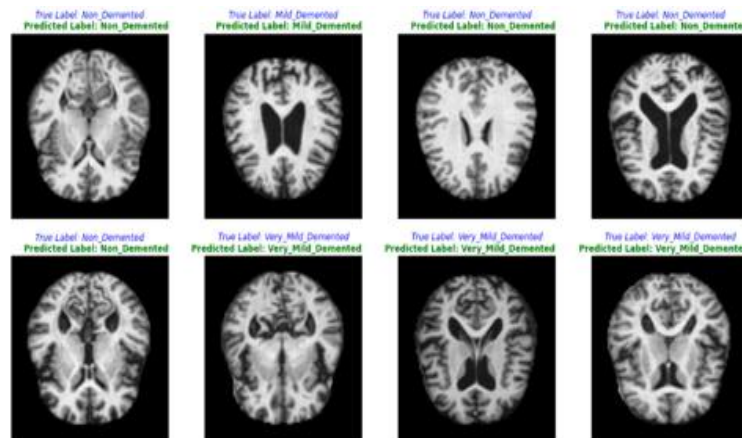Figure 10. Train and validation loss, accuracy

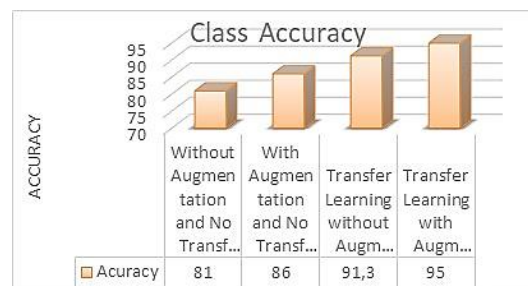Figure 11. Predictions between true label vs predicted label

Figure 12. Comparison of average class accuracy between different models

Table 5. Interpretations over existing and proposed model

Method	Dataset	Acc (%)	Generalizability	Efficiency	Pros	Cons
Traditional CNNs	ADNI, OASIS	80-85	Moderate	High	Strong pattern recognition	Requires large training data
Pre-trained CNNs (VGG, ResNet)	ADNI, AIBL	85-90	Moderate-high	Medium	Improved accuracy, feature reuse	May overfit to pre-trained features
Hybrid CNN-RNN	ADNI, OASIS	88-92	High	Medium	Captures sequential patterns	Computationally expensive
Attention-based networks	ADNI, AIBL	90-93	High	Medium-high	Focuses on key regions	Requires complex tuning
Proposed TL-AzNet	ADNI, OASIS	94-96	Very High	Optimized	High accuracy, robust to dataset variations	Potential for further real-world validation

4. CONCLUSION

AD is a prolonged degenerative disease. We have introduced a practical approach to leveraging brain MRI data for the detection of AD. While most existing research focuses on binary classification, our new model TL-AzNet with VGG19 base model provides a building model to classify multiclass. We think the suggested approach can be effectively applied to other classification problems in the medical field, even if it has only been evaluated on the AD dataset. The suggested model can be assessed in the future utilizing various AD datasets called multi-modality datasets, such as OASIS and other neurological disorder diagnoses. There were specific pros and cons of the proposed technique. Still, this model requires more features extracted from all model layers. Even in view of the suggested model's excellent performance in comparison to other CNN models.

ACKNOWLEDGEMENTS

AUTHOR CONTRIBUTIONS STATEMENT

This journal uses the Contributor Roles Taxonomy (CRediT) to recognize individual author contributions, reduce authorship disputes, and facilitate collaboration.

Name of Author	C	M	So	Va	Fo	I	R	D	O	E	Vi	Su	P	Fu
Pothala Ramya	✓	✓	✓	✓	✓	✓		✓	✓	✓	✓			
Chappa Ramesh			✓	✓		✓	✓	✓		✓		✓		
Odugu Srinivasa Rao			✓	✓		✓	✓			✓		✓		

C : **C**onceptualization		I : **I**nvestigation		Vi : **Vi**sualization	
M : **M**ethodology		R : **R**esources		Su : **Su**pervision	
So : **So**ftware		D : **D**ata Curation		P : **P**roject administration	
Va : **Va**lidation		O : Writing - **O**riginal Draft		Fu : **Fu**nding acquisition	
Fo : **Fo**rmal analysis		E : Writing - Review & **E**diting			

CONFLICT OF INTEREST STATEMENT

If there are no conflicts of interest, please include the following author's statement: Authors state no conflict of interest.

DATA AVAILABILITY

The data that support the findings of this study is available in AD Neuroimaging Initiative (ADNI) dataset. The data is not provided in this repository and needs to be requested directly from ADNI.

REFERENCES

[1] S. E. Pape, R. A. Baksh, C. Startin, S. Hamburg, R. Hithersay, and A. Strydom, "The association between physical activity and camdex-ds changes prior to the onset of alzheimer's disease in down syndrome," *Journal of Clinical Medicine*, vol. 10, no. 9, p. 1882, Apr. 2021, doi: 10.3390/jcm10091882.

[2] F. Nabizadeh, "sTREM2 is associated with attenuated tau aggregate accumulation in the presence of amyloid-β pathology," *Brain Communications*, vol. 5, no. 6, 2023, doi: 10.1093/braincomms/fcad286.

[3] A. P. Porsteinsson, R. S. Isaacson, S. Knox, M. N. Sabbagh, and I. Rubino, "Diagnosis of early Alzheimer's disease: clinical practice in 2021," *Journal of Prevention of Alzheimer's Disease*, vol. 8, no. 3, pp. 371–386, Jul. 2021, doi: 10.14283/jpad.2021.23.

[4] "2023 Alzheimer's disease facts and figures," *Alzheimer's and Dementia*, vol. 19, no. 4, pp. 1598–1695, Mar. 2023, doi: 10.1002/alz.13016.

[5] A. D. Arya *et al.*, "A systematic review on machine learning and deep learning techniques in the effective diagnosis of Alzheimer's disease," *Brain Informatics*, vol. 10, no. 1, Jul. 2023, doi: 10.1186/s40708-023-00195-7.

[6] D. A. Arafa, H. E. D. Moustafa, H. A. Ali, A. M. T. Ali-Eldin, and S. F. Saraya, "A deep learning framework for early diagnosis of Alzheimer's disease on MRI images," *Multimedia Tools and Applications*, vol. 83, no. 2, pp. 3767–3799, May 2024, doi: 10.1007/s11042-023-15738-7.

[7] R. Khan *et al.*, "A transfer learning approach for multiclass classification of Alzheimer's disease using MRI images," *Frontiers in Neuroscience*, vol. 16, Jan. 2023, doi: 10.3389/fnins.2022.1050777.

[8] H. A. Helaly, M. Badawy, and A. Y. Haikal, "Deep learning approach for early detection of Alzheimer's disease," *Cognitive Computation*, vol. 14, no. 5, pp. 1711–1727, Nov. 2022, doi: 10.1007/s12559-021-09946-2.

[9] N. An, H. Ding, J. Yang, R. Au, and T. F. A. Ang, "Deep ensemble learning for Alzheimer's disease classification," *Journal of Biomedical Informatics*, vol. 105, p. 103411, May 2020, doi: 10.1016/j.jbi.2020.103411.

[10] D. Nguyen *et al.*, "Ensemble learning using traditional machine learning and deep neural network for diagnosis of Alzheimer's disease," *IBRO Neuroscience Reports*, vol. 13, pp. 255–263, Dec. 2022, doi: 10.1016/j.ibneur.2022.08.010.

[11] P. Zhang, S. Lin, J. Qiao, and Y. Tu, "Diagnosis of Alzheimer's disease with ensemble learning classifier and 3D convolutional neural network," *Sensors,* vol. 21, no. 22, p. 20217634, doi: 10.3390/s21227634.

[12] F. Mohammad and S. Al Ahmadi, "Alzheimer's disease prediction using deep feature extraction and optimization," *Mathematics*, vol. 11, no. 17, p. 3712, Aug. 2023, doi: 10.3390/math11173712.

[13] G. I. Stoleru and A. Iftene, "Transfer learning for Alzheimer's disease diagnosis from MRI slices: a comparative study of deep learning models," *Procedia Computer Science*, vol. 225, pp. 2614–2623, 2023, doi: 10.1016/j.procs.2023.10.253.

[14] S. Afzal *et al.*, "A data augmentation-based framework to handle class imbalance problem for Alzheimer's stage detection," *IEEE Access*, vol. 7, pp. 115528–115539, 2019, doi: 10.1109/ACCESS.2019.2932786.

[15] N. Raza, A. Naseer, M. Tamoor, and K. Zafar, "Alzheimer disease classification through transfer learning approach," *Diagnostics*, vol. 13, no. 4, p. 801, Feb. 2023, doi: 10.3390/diagnostics13040801.

[16] C. Balaji and S. Veni, "Automatic skull stripping from mRI of human brain using deep learning framework for the diagnosis of brain related diseases," *International Journal of Intelligent Systems and Applications in Engineering*, vol. 11, no. 4, 2023.

[17] Z. Zhao, P. S. Q. Yeoh, J. H. Chuah, C. O. Chow and K. W. Lai, "Vision transformer-equipped convolutional neural networks for automated Alzheimer's disease diagnosis using 3D MRI scans," *Frontiers in Neurology*, vol. 15, doi: 10.3389/fneur.2024.1490829.

[18] H. Wang, C. Lei, D. Zhao, L. Gao, and J. Gao, "DeepHipp: accurate segmentation of hippocampus using 3D dense-block based on attention mechanism," *BMC Medical Imaging*, vol. 23, no. 1, Oct. 2023, doi: 10.1186/s12880-023-01103-5.

[19] A. Shukla, R. Tiwari, and S. Tiwari, "ALZ-CONVNets for classification of Alzheimer disease using transfer learning approach," *SN Computer Science,* vol. 4 no. 4, 2023, doi: 10.1007/s42979-023-01853-7.

[20] C. R. Nagarathna and M. Kusuma, "Automatic diagnosis of Alzheimer's disease using hybrid model and CNN," *Journal of Soft Computing Paradigm*, vol. 3, no. 4, pp. 322–335, Jan. 2022, doi: 10.36548/jscp.2021.4.007.

[21] L. Alzubaidi *et al.*, *Review of deep learning: concepts, CNN architectures, challenges, applications, future directions*, vol. 8, no. 1. Springer International Publishing, 2021.

[22] C. Shorten and T. M. Khoshgoftaar, "A survey on image data augmentation for deep learning," *Journal of Big Data*, vol. 6, no. 1, 2019, doi: 10.1186/s40537-019-0197-0.

[23] L. Pei *et al.*, "A general skull stripping of multiparametric brain MRIs using 3D convolutional neural network," *Scientific Reports*, vol. 12, no. 1, Jun. 2022, doi: 10.1038/s41598-022-14983-4.

[24] M. Leela, K. Helenprabha, and L. Sharmila, "Prediction and classification of Alzheimer disease categories using integrated deep transfer learning approach," *Measurement: Sensors*, vol. 27, p. 100749, Jun. 2023, doi: 10.1016/j.measen.2023.100749.

[25] R. Hedayati, M. Khedmati, and M. Taghipour-Gorjikolaie, "Deep feature extraction method based on ensemble of convolutional auto encoders: Application to Alzheimer's disease diagnosis," *Biomedical Signal Processing and Control*, vol. 66, p. 102397, Apr. 2021, doi: 10.1016/j.bspc.2020.102397.

BIOGRAPHIES OF AUTHORS

Pothala Ramya is research scholar at JNTUK Kakinada in Department of Computer Science and Engineering, working as Assistant Professor in MVGE College of Engineering (A), Andhara Pradesh, India. Her area of research are machine learning and image processing. She can be contacted at email: pothalaramya.583@gmail.com.

Dr. Chappa Ramesh professor, Department of Computer Science and Engineering, AITAM, Tekkali Srikakulam (Dt), Andhra Pradesh, India. His Areas of Interest: image processing, data mining, machine learning, computer networks. He Published papers in several National and International Journals and also organized several National and International Conferences. He can be contacted at email: chappa_ramesh01@yahoo.co.in.

Dr. Odugu Srinivasa Rao professor, Department of Computer Science and Engineering, University College of Engineering(A), Kakinada, JNTUK, Kakinada, Andhra Pradesh, India. His Area of Interest: cryptography, image processing, computer networks. He Published papers in several National and International Journals and also organized several National and International Conferences. He can be contacted at email: osr_phd@yahoo.com.